



**Direct Radiative Forcing Due to Aerosol Properties at the Peruvian
Antarctic Station And Metropolitan Huancayo Area**

Forçamento Radiativo Direto devido a Propriedades de Aerossóis na
Estação Antártica Peruana e na Área Metropolitana de Huancayo

Julio Miguel Angeles Suazo^{1,2}; Luis Suarez Salas³; Alex Rubén Huaman De La Cruz^{4,5};
Roberto Angeles Vasquez⁴; Georgynio Rosales Aylas⁶; Alicia Rocha Condor⁷; Edilson
Requena Rojas⁸; Felipa Muñoz Ccuro⁹; Jose Luis Flores Rojas³ & Hugo Abi Karam¹⁰

¹Universidad Nacional Intercultural de la Selva Central Juan Santos Atahualpa, Escuela Profesional
de Ingeniería Ambiental. Av. Perú 612, Pampa del Carmen, 12856 Chanchamayo, Perú.

²Universidad Tecnológica del Perú. Facultad de Ingeniería Civil, Av. Circunvalación 449, 12002 El Tambo, Huancayo, Perú.

³Instituto Geofísico del Perú, Calle Badajoz, 169, 15498 Urb. Mayorazgo IV Etapa, – Ate, Lima, -Perú

⁴Universidad Nacional del Centro del Perú, Instituto General de Investigación,
Av. Mariscal Castilla N° 3909, El Tambo, Huancayo, Perú.

⁵Universidad Católica los Ángeles de Chimbote, Instituto de Investigación, Jirón Tumbes N 247, Chimbote, Perú

⁶Universidade Federal do Espírito Santo, Engenharia Ambiental, Vitória, Av. Fernando Ferrari, 514- Goiabeiras, Vitória, ES, Brasil

⁷Universidad Alas Peruanas. Escuela Profesional de Ingeniería Ambiental. Av. Tacna 399, 12006, - Pilcomayo, Huancayo, Perú.

⁸Universidad Continental, Grupo de Investigación Multidisciplinario Ambiental, Avenida San Carlos 1980, Huancayo, Perú.

⁹Universidad Nacional Federico Villareal, Posgrado de Derecho, Jr. Carlos González 285 Urb. Maranga - San Miguel-Perú

¹⁰Universidade Federal do Rio de Janeiro, - Instituto de Geociências, – Departamento de Meteorologia, . Rua Athos
da Silveira Ramos 274, . Cidade Universitária, – Ilha do Fundão, –21.941-916, . Rio de Janeiro, -RJ, Brasil

E-mails: julio_as_1@hotmail.com; lsuarez@igp.gob.pe; alebut2@hotmail.com; roanvas@hotmail.com; ragy3008@gmail.com;
alicia.rocho.condor@hotmail.com; edilson.requena@gmail.com; w_munozcc@hotmail.com; jlflores@igp.gob.pe; hugo@igeo.ufrj.br

Recebido em: 29/05/2020 Aprovado em: 01/10/2020

DOI: http://dx.doi.org/10.11137/2020_4_404_412

Abstract

We describe the results of the study of aerosol optical depth (AOD) and Direct Radiative Forcing (DRF) in Top Of Atmosphere (TOA), obtained from the measurement and monitoring campaign carried out during the XXI Antarctic Peruvian Expedition in the months of January and February 2013 and in the Metropolitan Huancayo Area in the months of June and July 2019. In the Scientific Peruvian Station at Antarctic “Machu Picchu” our used a SP02-L sun photometer, which is within the instrumental framework of the International Polar Year. This instrument has 4 channels: 412 nm, 500 nm, 675 nm and 862 nm, thus allowing direct radiation spectra measurements. And in the MHA we used the BF5 sensor. This instrument measured Direct, Diffuse and Global Radiation in low wavelength. The results calculated of AOD in polar latitudes varied between 0.0646 to 0.1061, in relation to AOD in MHA, presents the value maximum that is 0.58 (11 of June) and minimum that is 0.19 (12 June). The Angstrom coefficient was determined have values ranging from 0 to 0.07, these values also indicates the presence of big particles. Also to the MHA presents the mean value varied from 0 to 1.8, that indicated the presence the aerosols types biomass burning and industrial. Recorded optical properties used to estimate the direct aerosol radiative forcing (DARF) at the top of the atmosphere. The results indicates that on King George Island site the DARF is between [-2 4] W/m²; also, the direct aerosol radiative forcing in MHA is between [0 20] W/m².

Keywords: *Aerosol, Radiative Forcing, Antarctic*

Direct Radiative Forcing Due to Aerosol Properties at the Peruvian Antarctic Station And Metropolitan Huancayo Area

Julio Miguel Angeles Suazo; Luis Suarez Salas; Alex Rubén Huaman De La Cruz; Roberto Angeles Vasquez; Georgynio Rosales Aylas; Alicia Rocha Condor; Edilson Requena Rojas; Felipa Muñoz Ccuro; Jose Luis Flores Rojas & Hugo Abi Karam

Resumo

Descrevemos os resultados do estudo da profundidade ótica do aerossol (POA) e do Forçamento Radiativo Direto (FRD) no topo da atmosfera (TOA), obtidos durante a campanha de medição e monitoramento, XXI Expedição Antártica do Peru, entre os meses de janeiro e fevereiro de 2013, e na área metropolitana de Huancayo (AMH) entre os meses de junho e julho de 2019. Na Estação Antártica Peruana Machu Picchu utilizou-se um fotômetro solar SP02-L. Tal instrumento possui 4 canais: 412 nm, 500 nm, 675 nm e 862 nm, permitindo realizar medições diretas do espectro de radiação visível. Na AMH usamos o sensor BF5, que mede a radiação direta, difusa e global em comprimento de onda curta. Os cálculos de AOD em latitudes polares variaram entre 0,0646 e 0,1061. Na AMH apresenta valor máximo de 0,58 (11 de junho) e mínimo de 0,19 (12 de junho). Determinou-se o coeficiente de Angstrom variando de 0 a 0,07, esses valores indicam a presença de partículas grandes. Na AMH varia de 0 a 1,8, que indica a presença de aerossóis de fonte de queima de biomassa e industrial. As propriedades óticas observadas foram usadas para estimar a forçante radiativa direta por aerossóis (FRDA) no topo da atmosfera. Os resultados indicam que no King George Island, o FRDA, está entre -2 e 4 W/m²; já para a AMH a forçante radiativa direta de aerossol está entre 0 e 20 W/m².

Palavras-chave: *Aerossol, Forçamento Radiativo, Antártico*

1 Introduction

As the direct solar radiation passes through the atmosphere, it is attenuated by two main physical processes: scattering (angular redistribution of energy) and absorption (conversion of energy into either heat or photochemical change). Both effects are known to be wavelength dependent (El-Shobokshy & Al-Saedi, 1993). Traditionally, the tool most commonly used for monitoring the aerosol optical depth of the atmosphere has been the sun photometer. Essentially, the instrument which is small in physical dimensions, is sighted at the sun to measure the direct solar irradiance in some selected narrow spectral intervals (Volz, 1959).

Aerosol particles affect the climate system via the following physical mechanisms: First, they scatter and can absorb solar radiation. Second, they can scatter, absorb and emit thermal radiation. Third, aerosol particles act as cloud condensation nuclei (CCN) and ice nuclei (IN). The first two mechanisms are referred to as direct effects and are not subject of this paper but are discussed in detail in e.g., Haywood & Boucher (2000). The last one is referred to as indirect effect. It will be the subject of this review together with other atmospheric properties influenced by aerosols (e.g. semi-direct effect, suppression of convection).

Even though the semi-direct effect is a consequence of the direct effect of absorbing aerosols, it changes cloud properties in response to these aerosols and therefore is part of this review on aerosol-cloud-interactions.

Radiative Forcing (RF) is defined as the change in net irradiance at the tropopause due to an applied perturbation holding all atmospheric variables fixed, once stratospheric temperatures have been allowed to adjust to equilibrium. The concept of RF was first developed for one-dimensional (1-D) radiative convective models (e.g., Houghton *et al.*, 1995) considered the direct radiative forcing from three

different anthropogenic aerosol species: sulphate, fossil fuel black carbon (or soot), and biomass-burning aerosols.

Houghton, *et al.* (1995), suggested a range of 20.2 to 20.8 W m⁻² (“best guess” of 20.4 W m⁻²) for sulphate aerosols, 10.03 to 10.3 W m⁻² (best guess of 10.1 W m⁻²) for fossil fuel black carbon aerosols, and 20.07 to 20.6 W m⁻² (best guess of 20.2 W m⁻²) for biomass-burning aerosols.

The present research work estimates the direct radiative forcing of aerosols at the Scientific Peruvian Station Antarctic Machu Picchu and in the Metropolitan Huancayo Area

2 Methods

2.1 Site description

The Scientific Peruvian Station at Antarctic “Machu Picchu” (referred as ECAMP, 62°05’30” S, 58°28’16” W and 6 meter above sea level (masl)) is located at King George Island, the largest of the South Shetland Islands, on the northern tip of the Antarctic peninsula (Figure 1). About 90% of King George Island extension is covered by ice (Simoes *et al.*, 1999). The Peruvian station is located very close to the open ocean so the climate regime is characterized by maritime conditions. Brazilian and Polish Antarctic stations are the closest ones. The Peruvian station is only operated during austral summer covering periods from December to March at maximum, depending of logistics aspects. This station is operated by the Peruvian Antarctic Institute and actually is run by the Office of Antarctic Affairs of the Ministry of External Affairs.

The closest station to Peruvian station with continuous meteorological measurements is Comandante Ferraz, the Brazilian Antarctic station that is about only 5 km from the Peruvian one. Temperature records for the period of 1947 to 1995 shows that the mean is -2.8°C, with a minimum of

-5.2°C and a maximum of -0.8°C, for year 1959 and 1989, respectively. It showed a warming trend of 0.022°C per year, resulting in a mean air temperature rise of 1.1°C over 49 years. The temperature during summer, the season that covers the aerosol sampling at the Peruvian station, could reach some degrees over 0°C, with a mean of 0.9°C (Ferron *et al.*, 2004). Storms are quite frequent over this region of the Antarctic Peninsula so mean wind speed is above 4 m/s with high variability due to synoptic circulation patterns like the next ones described by Braun *et al.* (2001):

- (a) advection from north to northwest
- (b) southerly to southeasterly air mass transport
- (c) advection from northwest
- (d) advection from west to southwest

The study was also conducted in the MHA located at coordinates 12°4'12.03''S, 75°12'43.55''W with altitude of 3300 masl, it is part of the central Andean region of Peru, as seen in Figure 2, located in South America and east of the Pacific Ocean. It is one of the 10 most populous provinces of Peru, whose annual population growth rate is 1.6%, with more than half a million inhabitants (Instituto Nacional de Estadística e Informática, 2007).

The MHA belongs to the Mantaro Valley, it occupies an area of 319.4 km². Its topography is quite complex with rock formations and altitudes ranging between 3000-5000 masl, this range of altitudes is generally due to the presence of mountains.

2.2 Instrument

Field campaigns for taking sun photometry measurements were carried during Peruvian Antarctic campaign: ANTAR XXI (January and February 2013) and Campaign in the Huancayo province (June and July 2019). The fieldwork at ECAMP and Huancayo has been programmed with the main objective of quantifying the AOD as an indicator of atmospheric pollution and evaluate its variation among the different years of measurements.

The main instrument used was the sun photometer that collects information about the physical and optical properties of aerosols along a vertical path of the atmosphere. This sun-photometer, named herein front as SP02-L, is used to measure solar irradiance at five different wavelengths that nominally are 412, 500, 675, 862 nm with 10 nm of bandpass (Middleton Solar, 2004). A previous model has been used extensively for other research groups by NOAA/USA (Stone, 2002), by the Australian Bureau of Meteorology in its national network (Mitchell & Forgan, 2003) and more recently by groups for doing measurements at Antarctic sites as part of a namely POLAR AOD network (Mazzola *et al.*, 2011). In this improved model it has a 35 mm longer body to give a narrower field of view of 2.5° (1.25° opening angle), a slope angle of 0.7° and a limit angle of 1.8°. The fieldwork at Huancayo the instrument used was the sun pyranometer, BF5 model; that collects

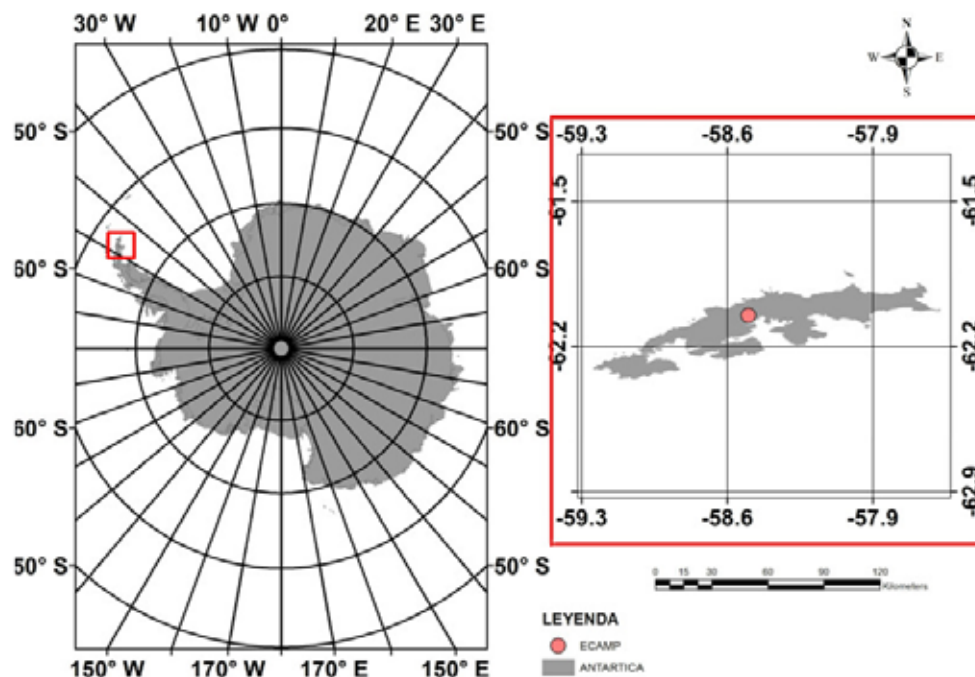


Figure 1 Map presenting the location of the Peruvian Antarctic Station “Machu Picchu” and the main geographical references.

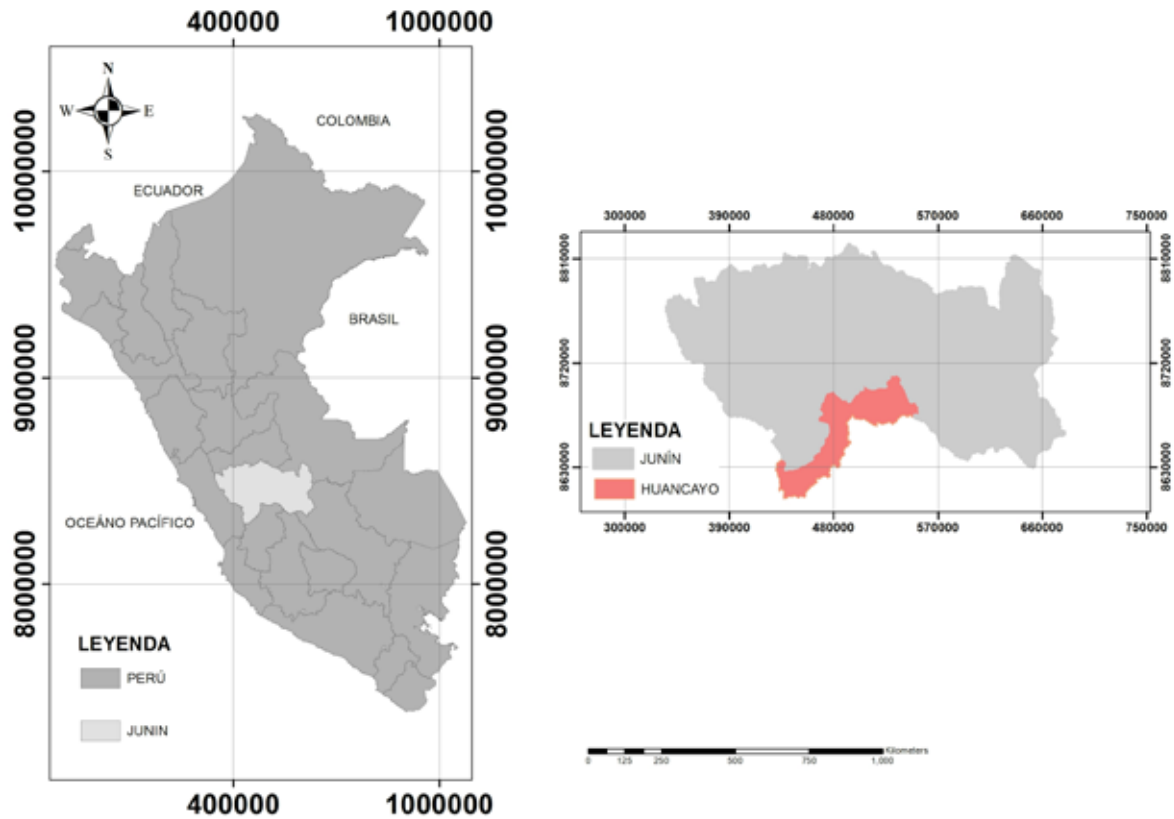


Figure 2 A. Location map of the Department of Junín in Peru; B. Geographic localization of the MHA; C. Topographical distribution of the MHA.

information about the diffuse and direct radiation along a vertical path of the atmosphere.

For the corresponding measurements of solar radiation in the Province of Huancayo, was used the BF5 sensor, located at $12^{\circ}4'0''$ S and $75^{\circ}13'0''$ W, in the Metropolitan Huancayo Area. This records data with a frequency interval every minute, of the following variables: global radiation and diffuse incident radiation since June at July, 2019. With this information, the atmospheric clarity index was determined, and the temporal variability was analyzed direct, diffuse and global solar radiation. The BF5 Sensor is a patented design. It uses a series of photodiodes with a unique computer-generated hatch pattern to measure incident solar radiation. A microprocessor calculates the Global and Diffuse components of solar radiation. A built-in heater keeps the BF5 free from dew, ice, and snow down to -20°C .

2.3 Aerosol Optical Depth

The direct solar irradiance measured with this sun-photometer is used to describe the spectral values of the aerosol optical depth (AOD) associated to each

wavelength that are determined based on the well known law of Lambert-Bouguer-Beer.

$$I(\lambda) = I_0(\lambda)R^{-2}e^{-m\tau(\lambda)} \quad (1)$$

Where $I(\lambda)$ is the solar intensity recorded at each wavelength λ , $I_0(\lambda)$ is the value of solar radiation at the top of the atmosphere (TOA), R is the solar distance expressed as astronomical units, m is the air optical mass and $\tau(\lambda)$ is the total optical depth dependent on wavelength. This last term can be described as the sum of the different constituents of the atmosphere.

$$\tau(\lambda) = \tau_a(\lambda) + \tau_R(\lambda) + \tau_{o_3}(\lambda) \quad (2)$$

Where $\tau_a(\lambda)$ is the aerosol optical depth, $\tau_R(\lambda)$ is the Rayleigh-Scattering optical depth, and $\tau_{o_3}(\lambda)$ is the ozone optical depth (Liou, 2007).

It should be noted that Equations 1 and 2 are used in the estimation of AOD for ECAMP.

For AMH, if the model established by Iqbal (1983) is used, the optical aerosol thickness can be estimated using the IQC model:

$$\tau_a = 0.2758x0.38^{-x} + 0.35x0.5^{-x}\beta \quad (3)$$

2.4 Angstrom exponent

Another important optical property of aerosols is the Ångström exponent (Ångström, 1964). It permits to quantify the spectral dependence of the AOD related with size and the vertical profile (Tomasi *et al.*, 1983). Ångström exponent is the slope of the lines that passes through the two values of AOD dependent of λ in a logarithmic scale as showed in equation 4 (World Meteorology Organization, 2005)

This indicator is very useful because high values of α indicate the predominance of fine particles and low values of α suggest the opposite. During this study it has been used 500 and 862 nm wavelengths accounting a small

difference related to the World Meteorological Organization suggestion of 870 nm.

$$\alpha = - \frac{\log \left(\frac{\tau_2}{\tau_1} \right)}{\log \left(\frac{\lambda_2}{\lambda_1} \right)} \quad (4)$$

For the calculation of the Angstrom exponent in MHA, it was based on the Iqbal Model, using parameterization techniques as mentioned in his research Flores *et al.* (2014).

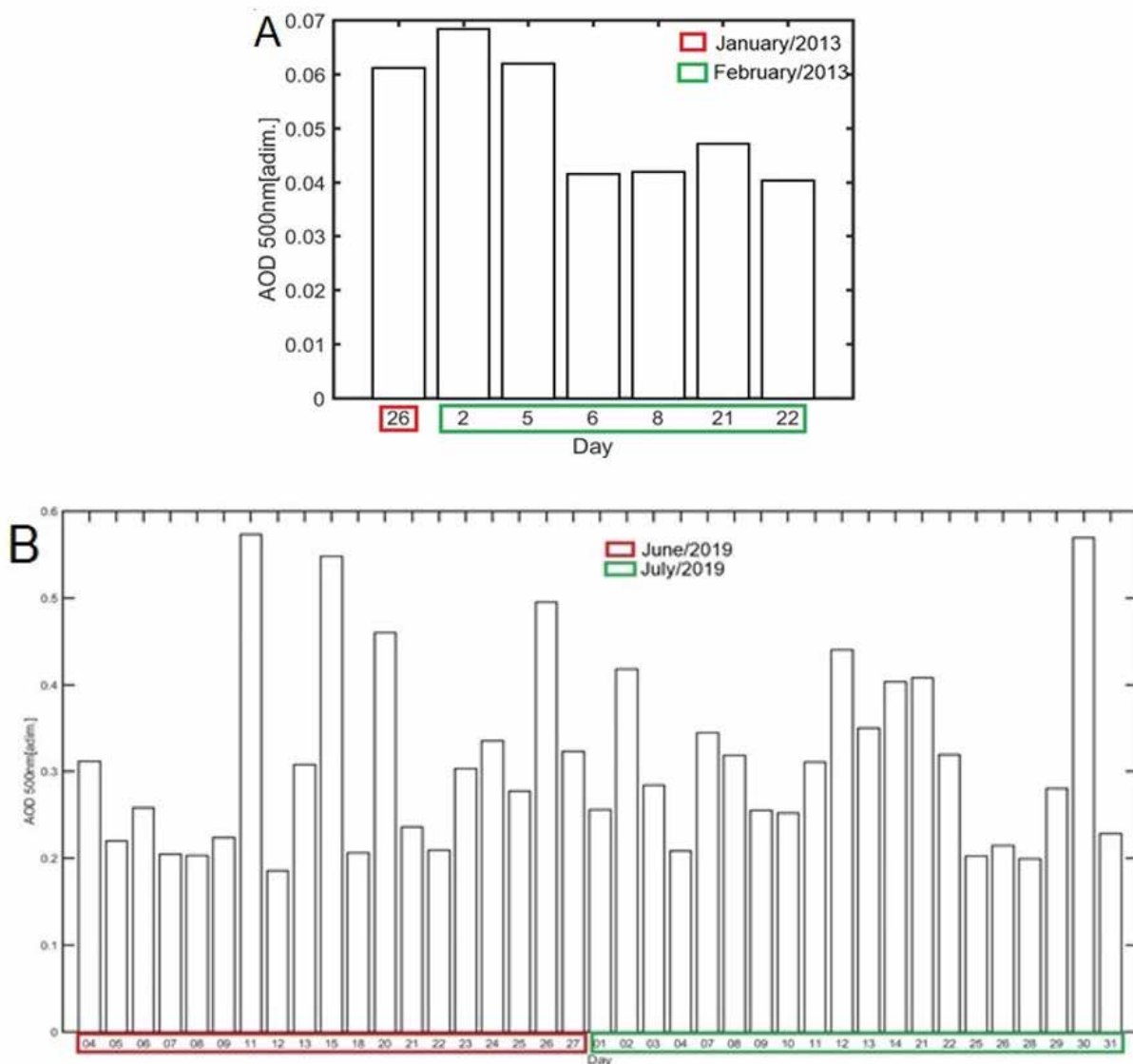


Figure 3 A. Daily variation of AOD at 500 nm for austral summers of 2013 in ECAMP; B. 2019 in MHA.

2.5 Direct Radiative Forcing

The attenuation of aerosols during clear sky conditions is known as the ‘direct’ influence of aerosols on climate. This effect results from backscattering and absorption of radiation by the aerosol particles themselves (Charlson *et al.*, 1992; Haywood & Boucher, 2000). Although many monitoring efforts the broad range of estimates due to aerosol direct radiative forcings still remains large and an important source of uncertainty in climate models (Forster *et al.*, 2007). Less data, spatially and temporal, is available at Polar regions. In that sense, as a globally-averaged annual mean, this direct attenuation will produce a cooling sign almost of the same magnitude of the warming caused by the greenhouse gases (Myhre & Shindell, 2013).

The annual mean at the top of the atmosphere direct shortwave aerosol radiative forcing, DF, can be roughly estimated using equation 6 and some values suggested by Haywood & Shine (1995).

$$\diamond F = -DS_oT_{at}^2(1 - Ac)\omega\beta\tau\left((1 - R_s)^2 - \frac{2R_s}{\beta}\left(\frac{1}{\omega} - 1\right)\right) \quad (5)$$

Where:

- D is the fractional day length (0.7 and 0.5 to ECAMP and MHA respectively),
- S_o is the solar constant (1370 Wm^{-2}),
- T_{at} the atmospheric transmission (0.76),
- Ac fractional cloud cover (0.6 and 0.35 to ECAMP and MHA respectively, based on the mean daily record of Cloud_Fraction from the Moderate Resolution Imaging Spectroradiometer (MODIS) sensor for King George Island site),
- R_s the surface reflectance (0.65 and 0.20 to ECAMP and MHA respectively, based on the mean daily record of Effective surface reflectivity at 360 nm (%) from Ozone Monitoring Instrument (OMI) sensor),
- ω , the single scattering albedo, 0.8 at 1 and calculate for Iqbal method (1983)
- β , the upscatter fraction (0.27, based on measurement of medium latitudes),
- τ , the aerosol optical depth,

3 Results

3.1 Aerosol Optical Depth

Records of AOD at polar latitudes shows the lowest values of the world with higher values at Arctic than Antarctic. Figure 3A shows the complete set of daily records of AOD during Peruvian Antarctic Campaigns at

ECAMP developed during austral summers of 2013. During these years AOD (500 nm) varied between 0.0646 to 0.1061, being a typical value for the conditions of atmospheric turbidity at a polar site dominated by maritime conditions, during this season of the year (Tomasi *et al.*, 2007), also are lower than the ones registered at urban cities, from 0.25 to 1.7 (Castro *et al.*, 2001), and much lower that records during biomass burning season where values can have values as high as 2.4 for the same wavelengths (Eck, 2003). Then the Figure 3B, in relation to AOD in MHA, presents the value maximum that is 0.58 (11 of June) and minimum that is 0.19 (12 June). Estevan *et al.* (2019) utilize a CIMEL sunphotometer belonging to the AERONET network have been performed in the Huancayo Observatory, Peru, from March 2015 to August 2017, two and a half years, providing for the first time information about aerosols in the specific area, and obtain the month with the maximum AOD monthly average is September, and in 2016, the absolute maximum value of 0.91 was registered. The mean AOD value for the study period is 0.10 ± 0.07 and the alpha mean value is 1.49 ± 0.36 , indicating presence, of small size aerosols.

Comparing these values with other Antarctic monitoring stations, the ECAMP ones presents a high median for AOD (500 nm) of 0.0781. AOD recorded at Neumayer and Aboa Stations were 0.06 and 0.0551, respectively. These sites are also very close to the coast where the influence of marine aerosols is higher. Continental sites, far from the coast, present lower values. AOD at Kohne and South Pole stations were values as low as 0.015 were recorded (Tomasi *et al.*, 2007).

The comparison between the ECAMP and the other station offers the evidence of the main and important differences of the optical properties of the aerosols. Polar sites has a relatively very clean atmosphere, but they have a strong influence of particles, very small, mainly of marine source and eventually from anthropogenic sources and to the turbidity conditions that is usually present in summer and fall because the strong prevailing winds that also transport haze and dust (Shaw, 1982).

3.2 Angstrom Coefficient

Angstrom coefficient α is useful to compare and characterize the wavelength dependence of AOD and columnar aerosol size distribution (Eck *et al.*, 1999; Cachorro *et al.*, 2001). Smaller values represent bigger particles, for example dust. On the other hand, higher values represent smaller particles like smoke and/or burning particles (Shifrin, 1995). One way to discriminate if the aerosols are mainly composed by particles of medium – small radius, smaller than 1 μm , or higher is to calculate the Ångström for the evaluated days. Values of α that are in

the range of 0.12 and 0.4 indicates the presence of particles of big size (Otero *et al.*, 2006), as it is shown in figure 4A from for the Antarctic site. During the year of campaign, the mean value for Angstrom coefficient (α) varied from 0 to 0.07 that represents a low variability that can be both to instrumental and atmospheric properties but also indicates the dominance of big particles probably coming from maritime source. Also to the MHA in figure 4B, presents the mean value for Angstrom coefficient (α) varied from 0 to 1.8, that indicated the presence the aerosols types biomass burning and industrial.

3.3 Aerosol Top Of Atmosphere (TOA) Aerosol Direct Radiative Forcing

The Aerosol TOA Aerosol Direct Radiative Forcing (ADRF) is strongly dependent of AOD (τ_a) and of single scattering albedo (SSA, ω_0), that it is a measure of scattering and absorption processes of solar light caused by aerosols becoming a key variable for ADRF determination.

Comparing the forcing estimates with AOD values, we find that the radiative forcing is primarily governed by the magnitude of AODs which varied from a low value

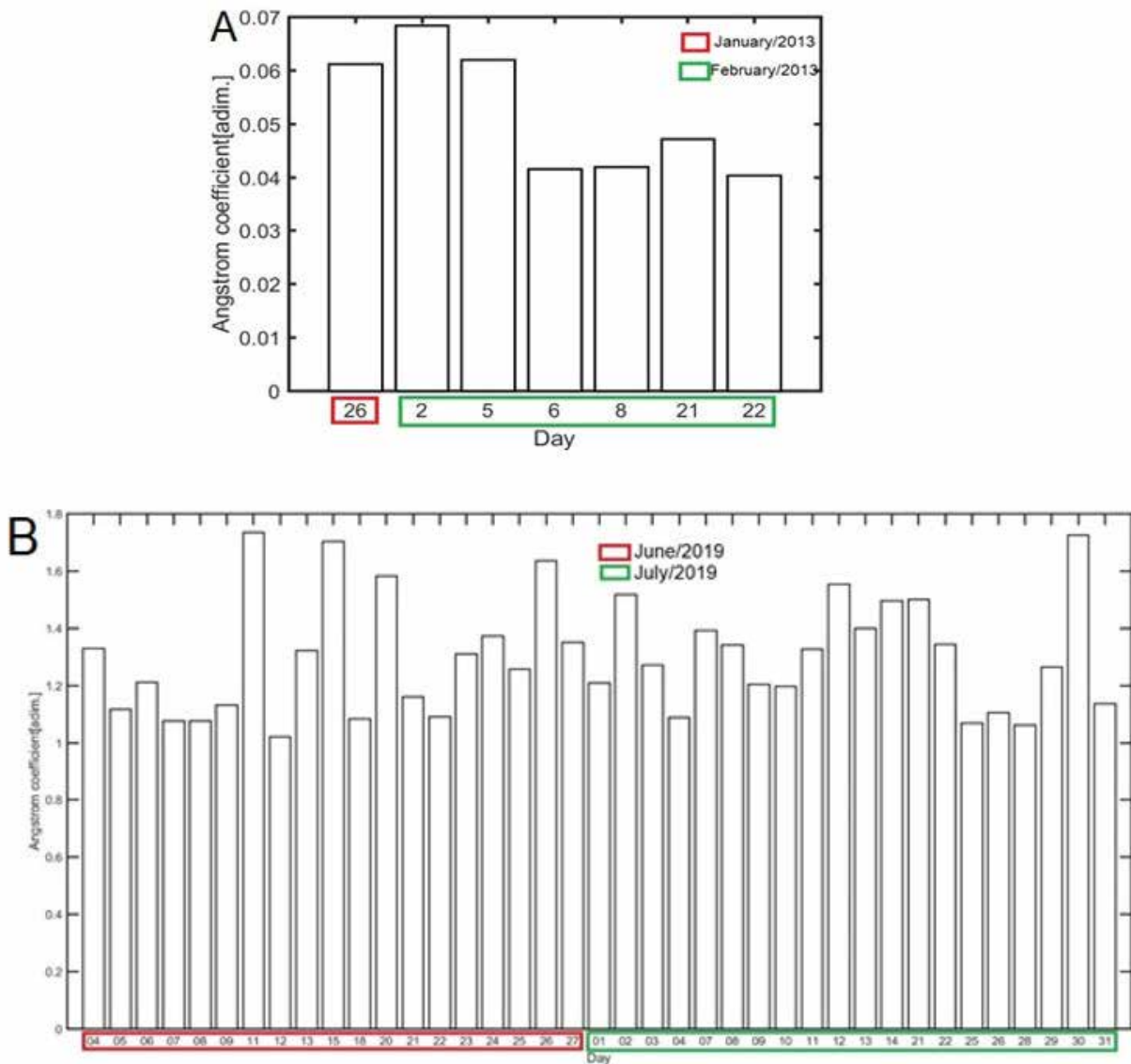


Figure 4 A. Daily Ångström exponent variations during Peruvian Antarctic Campaigns at ECAMP for year 2013 and B. MHA for year 2019.

of 0.04 to high values above 0.065 at 0.5 μm during the field campaigns.

For evaluating and estimating the ADRF it was used the median of AOD (at 500 nm) as it is the most representative value due to this non-parametric distribution. Our estimation for the King George Island site suggests that

based on the equation 5 the direct aerosol radiative forcing is between $[-2\ 4]\ \text{W/m}^2$. The figure 5B shows the variation of the ADRF based on the optical properties determined in the MHA, also the direct aerosol radiative forcing is between $[0\ 20]\ \text{W/m}^2$

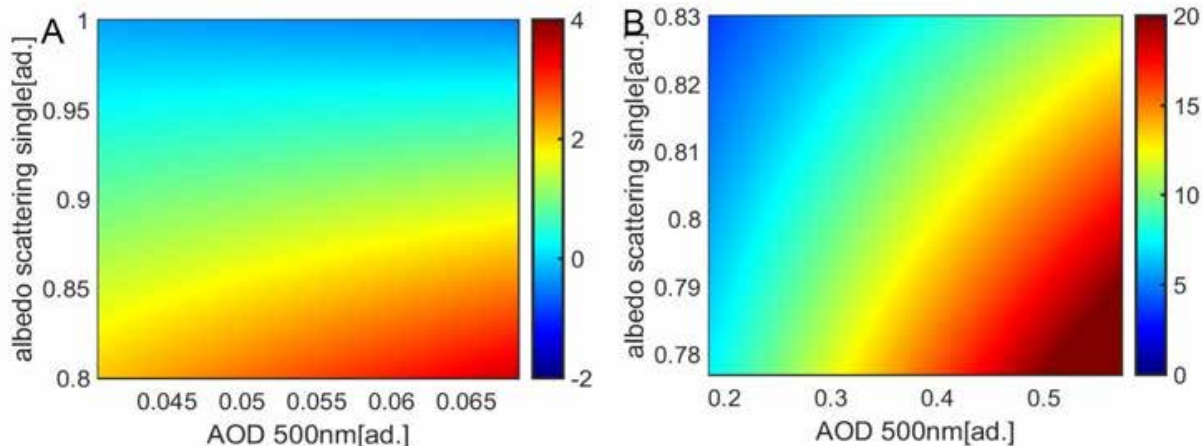


Figure 5 A. Dependence of single scattering albedo (ω) and AOD on the direct aerosol radiative forcing (ADRF) for King George Island and B. MHA.

4 Conclusions

Measurements of optical properties of aerosols performed during Peruvian Antarctic campaigns of year 2013 and MHA of year 2019 were analyzed; during these years AOD (500 nm) varied between 0.0646 to 0.1061, in relation to AOD in MHA, presents the value maximum that is 0.58 (11 of June) and minimum that is 0.19 (12 June).

The Angstrom coefficient was determined by the same years with values ranging from 0 to 0.07 presenting a high variability that can be both to instrumental and atmospheric aspects. These values also indicate the presence of big particles. Also to the MHA presents the mean value for Angstrom coefficient (α) varied from 0 to 1.8, that indicated the presence the aerosols types biomass burning and industrial.

It was evaluated a first inference about the role of aerosols on the Earth's energy balance. Recorded optical properties were used to estimate ARDF at the top of the atmosphere. The results indicate that focusing on King George Island site the ARDF is between $[-2\ 4]\ \text{W/m}^2$. Also, the direct aerosol radiative forcing in MHA is between $[0\ 20]\ \text{W/m}^2$.

5 Acknowledgement

Authors thanks to the Ministerio de Relaciones Exteriores-Perú, especially to the Dirección de Asuntos

Antarticos by financial support and equipment provided in the 2013.

6 References

- Ångström, A. 1964. The parameters of atmospheric turbidity. *Tellus*, 16: 64-75.
- Braun, M.; Saurer, S.; Vogt, J.; Simoes, C. & Gobmann, H. 2001. The influence of large-scale atmospheric circulation on the surface energy balance of the King George Island ice cap. *International Journal of Climatology*, 21: 21–36.
- Cachorro, V.; Vergaz, R. & Frutos, A. 2001. A quantitative comparison of a-Angstrom turbidity parameter retrieved in different spectral ranges based on spectroradiometer solar radiation measurements. *Atmospheric Environment*, 35: 5117– 5124.
- Castro, T.; Madronich, S.; Rivale, S.; Muhlia, A. & Mar, B. 2001. Influence of aerosols on photochemical smog in Mexico City. *Atmospheric Environment*, 35: 1765-1772.
- Charlson, R.; Schwartz, S.; Hales, J.; Cess, R.; Coakley, J.; Hanes, J. & Hofmann, D. 1992. Climate forcing by anthropogenic aerosols. *Science*, 255: 423–430.
- Eck, T.; Holben, B.; Reid, J.; O'Neill, N.; Schafer, J.; Dubovik, O.; Simimov, A.; Yamasoe, M. & Artaxo, P. 2003. High aerosol optical depth biomass burning events: A comparison of optical properties for different source regions. *Geophysical Research Letters*, 30(20): 2035-2044.
- Eck, T.F.; Holben, B.N.; Reid, J.S.; Dubovik, O.; Smirnov, A.; O'Neill, N.; Slutsker, I. & Kinne, S. 1999. Wavelength dependence of the optical depth of biomass burning, urban,

Direct Radiative Forcing Due to Aerosol Properties at the Peruvian Antarctic Station And Metropolitan Huancayo Area

Julio Miguel Angeles Suazo; Luis Suarez Salas; Alex Rubén Huaman De La Cruz; Roberto Angeles Vasquez; Georgynio Rosales Aylas; Alicia Rocha Condor; Edilson Requena Rojas; Felipa Muñoz Ccuro; Jose Luis Flores Rojas & Hugo Abi Karam

- and desert dust aerosols. *Journal of Geophysical Research*, 104(31): 333– 349.
- Estevan, R.; Martínez, D.; Suarez, L.; Moya, A. & Silva, Y. 2019. First two and a half years of aerosol measurements with an AERONET sunphotometer at the Huancayo Observatory, Peru. *Atmospheric Environment*, 3: 1-13.
- El-Shobokshy, M. & Al-Saedi, Y. 1993. Atmospheric turbidity and transmittance of solar radiation in Riyadh, Saudi Arabia. *Atmospheric Environment*, 27(4): 401–411.
- Ferron, F.; Simões, J.; Aquino, F. & Setzer, A. 2004. Air temperature time series for King George Island, Antarctica. *Pesquisa Antártica Brasileira*, 4: 155-169.
- Forster, P.; Ramaswamy, V.; Artaxo, P.; Berntsen, T.; Betts, R.; Fahey, D. W.; Haywood, J.; Lean, J.; Lowe, D. C.; Myhre, G.; Nganga, J.; Prinn, R.; Raga, G.; Schulz, M. & Van Dorland, R. 2007. Changes in Atmospheric Constituents and Radiative Forcing, In: Climate Change 2007: The Physical Science Basis, Contribution of Working Group I to the Fourth Assessment Report of the Intergovernmental Panel on Climate Change. Cambridge University Press, Cambridge, UK and New York, NY, USA.
- Haywood, K. & Shine, K. 1995. The effect of anthropogenic sulfate and soot aerosol on the clear sky planetary radiation budget. *Geophysical Research Letters*, 22(5): 603-606.
- Haywood, J. & Boucher, O. 2000. Estimates of the direct and indirect radiative forcing due to tropospheric aerosols: a review. *Reviews of Geophysics*, 38(4): 513-543.
- Instituto Nacional de Estadística e Informática. 2007. Perfil sociodemográfico de la provincia de Huancayo. Disponible en: https://www.inei.gob.pe/media/MenuRecursivo/publicaciones_digitales/Est/Lib1136/libro.pdf. Acceso en 2 de febrero de 2020 y 1 de junio de 2020.
- Houghton, J.; Moreira, L.; Callander, B.; Harris, N.; Kattenberg, A. & Maskell, K. 1995. *Climate Change 1995: The Science of Climate Change, The Contribution of Working Group I to the Second Assessment Report of the IPCC*. New York, Cambridge University Press, 572p.
- Liou, K. 2007. *An introduction to atmospheric radiation*. New York 2nd Ed., Academic Press, 583p.
- Mazzola, M.; Stone, R.S.; Herber, A.; Tomasi, C.; Lupi, A.; Vitale, V.; Lanconelli, C.; Toledano, C.; Cachorro, V.; O'Neill, N.; Shiobara, M.; Aaltonen, V.; Stebel, K.; Zielinski, T.; Petelski, T.; Ortiz de Galisteo, J.; Torres, B.; Berjon, A.; Goloub, P.; Li, Z.; Blarel, L.; Abboud, I.; Cuevas, E.; Stock, M.; Schulz, K. & Virkkula, A. 2011. Evaluation of sun photometer capabilities for retrievals of aerosol optical depth at high latitudes: The POLAR-AOD intercomparison campaigns. *Atmospheric Environment*, 52: 4-17.
- Myhre, G. & Shindell, D. 2013. *Anthropogenic and Natural radiative Forcing*. Intergovernmental Panel of Change Climate, p. 659-740.
- Middleton Solar. 2004. SP02 y SP02-L Sunphotometer user's guide, Victoria, pag. 9.
- Mitchell, R. & Forgan, B. 2003. Aerosol measurement in the Australian outback: intercomparison of sun photometers. *Journal of Atmospheric and Oceanic Technology*, 20: 54-66.
- Otero, L.; Ristori, P.; Holben, B. & Quel, E. 2006. Espesor óptico de aerosoles durante el año 2002 para diez estaciones pertenecientes a la red AERONET – NASA. *Óptica Pura y Aplicada*, 39(4): 355-364.
- Shaw, G. 1982. Atmospheric turbidity in the Polar regions. *Journal of Applied Meteorology*, 21: 1080– 1088.
- Shifrin, K. 1995. Simple Relationships for the Angstrom parameter of disperse systems. *Applied Optical*, 34: 4480 – 4485.
- Simoes, J.; Bremer, U.; Aquino, F. & Ferron, F. 1999. Morphology and variations of glacial drainage basins in the King George Island ice field, Antarctica. *Annals of Glaciology*, 29: 220– 224.
- Stone, R.S. 2002. Monitoring aerosol optical depth at Barrow, Alaska and South Pole; Historical overview, recent results, and future goals. In: COLACINO, M. (ED.), Proceedings of the 9th Workshop Italian Research on Antarctic Atmosphere, Rome, Italy, 22-24 October 2001. Italian Physical Society, Bologna, Italy, pp. 123-144.
- Tomasi, C.; Caroli, E. & Vitale, V. 1983. Study of the relationship between Ångström's wavelength exponent and Junge particle size distribution exponent. *Journal of Climate and Applied Meteorology*, 22: 1707-1716.
- Tomasi, C.; Vitale, V.; Lupi, A.; Di Carmine, C.; Campanelli, M.; Herber, A.; Treffeisen, R.; Stone, R.; Andrews, E.; Sharma, S.; Radionov, V.; von Hoyningen-Huene, W.; Stebel, K.; Hansen, G.H.; Myhre, C.; Wehrli, C.; Aaltonen, V.; Lihavainen, H.; Virkkula, A.; Hillamo, R.; Ström, J.; Toledano, C.; Cachorro, V.; Ortiz, P.; de Frutos, A.; Blindheim, S.; Frioud, M.; Gausa, M.; Zielinski, T.; Petelski, T. & Yamanouchi, T. 2007. Aerosols in polar regions: a historical overview based on optical depth and in situ observations. *Journal of Geophysical Research*, 112: 1-28.
- Volz, F. 1959. Photometer mit Selen-Photoelement zur spektralen messung der Soonenstrahlung and zur Bestimmung der wellenlangenabhängigkeit der Dunsttrübung. *Archiv fur Meteorologie Geophysik und Bioklimatologie*, 10: 100-131.
- World Meteorology Organization. 2005. *WMO/GAW Experts Workshop on a Global Surface-based Network for Long Term Observations of Column Aerosol Optical Properties*. Switzerland, 153 p.